ISSN (e): 2250 – 3005 || Volume, 08 || Issue, 4|| April – 2018 ||
International Journal of Computational Engineering Research (IJCER)

Strata movement and stress evolution when mining two overlapping panels affected by hard stratum

Alok Sunder Mohanty [1] Aliva Mohanty[2] Goutam Mishra [3] Dr. K. C. Singh[4]
Department of Mechanical Engineering,Aryan Institute of Engineering & Technology, Bhubaneswar
Department of Mechanical Engineering, Raajdhani Engineering College, Bhubaneswar
Department of Mechanical Engineering, Capital Engineering College, Bhubaneswar
Department of Mechanical Engineering, NM Institute of Engineering & Technology, Bhubaneswar

ABSTRACT: *Mining causes stress redistribution and stratum movement. In this paper, a numerical model was built according to the geological conditions in the 12th coal mine in Pingdingshan city to study the strata movement and the evolution of stress when mining two overlapping longwall panels, named panels #14 and #15. The strata close to the mined panel move directly towards the gob, while the strata that are farther away swing back and forth during the mining process. The directed movement and swinging can break the transverse boreholes for gas extraction; a surface borehole should not be within the range of directional movement. The stress evolution suggested that the mining of the lower panel #15 after the upper panel #14 would further increase the de-stressed range, while the stress concentration around the mined panel would be increased. Hard strata usually carry a greater stress than adjacent rocks and soft coal seams. The stress in a hard stratum increases greatly, and the stress decreases greatly in the coal seams below the hard stratum. This study supplies a reference for similar coal mines and is useful for determining the de-stressed range and transverse borehole arrangement for gas extraction.*

I. INTRODUCTION

Deep coal seams usually bear a higher ground stress and a higher gas content than shallow coal seams, which increases the risk of gas outburst, and most coal seams deeper than 500 m are prone to dangerous gas release [1–3]. To reduce the risk of explo- sion, the development of a safety coal seam as a measure of protec- tion is a method that is widely used all over the world. The redistribution of stresses and the movement of surrounding rocks during mining a protective coal seam is important for determining the pressure relief range and the location of the borehole to extract gas for pressure relief [4,5]. The recommended upper and lower pressure relief limits when mining a protective coal seam with a slope below 25°, according to Chinese law, are 100 m and 50 m, respectively, and coal mining enterprises are encouraged to study their own accurate parameters. However, in deep coal mines, methods for determining the pressure relief zone have been studied less extensively.

Rock strata movement in the vertical direction is widely studied [6–8]. The roof was divided into three zones in the vertical direc- tion, including the cave zone, the fractured zone, the original zone, and three zones in the horizontal direction, including the abutment stress concentration zone, pressure relief zone, and pressure recov- ery zone [9,10]. The boundaries of the zones are different in differ- ent rock strata, and currently there is no proper method to clearly identify the boundaries. Physical laboratory models were used to study the roof movement, and then identify the boundaries [11]; however, laboratory models are typically in 2D and cannot be used to represent the real conditions. The de-stressed range was also tested by a field experiment, which is an intuitive method for studying the evolution and distribution of pressure [12–14]; how- ever, the testing points are usually insufficient and sometimes very difficult to determine. Roof movements caused by hard and thick sandstone were also investigated [15–17], which was helpful for studying the abnormal characteristics of the gas flow and extrac- tion. The structural characteristics of key strata and strata behavior when mining a thick coal seam were also examined, and the results proved useful for determining the working resistance [18]. Numer- ical modelling using elastic finite and boundary element methods was performed to analyze the stress redistribution, strata failure, and water inflow enhancements that result from these coal mining operations [19,20].

In general, monitoring parameters is the most difficult aspect of laboratory or field experiments, and it is difficult to monitor stress or movement in the inner coal or rock. Numerical simulation is one of the most appropriate methods for underground studies and is widely used in underground engineering [21]. Both physical and numerical models are simplified, because it is usually difficult to construct a large and sufficiently accurate model to represent the original geological conditions and stress field. In addition, there are usually several coal seams in one coal mine; for example, there are five valuable coal seams in the Pingdingshan coal field. Mining of several coal seams can lead to a complex stress evolution, which will greatly affect the de-stressed range [22]. Mining of several coal seams will also cause complex strata movement in both the verti- cal and horizontal directions. Rock strata usually differ in hardness, which also leads to complication of the stress evolution and strata movement.

In this paper, we construct a numerical model according to the real geological conditions of the 12th coal mine in Pingdingshan and verify the model based on field results to study the stress evo- lution and strata movement when mining several overlapping longwall panels. The evolution of stress and the vertical stratum movement are helpful for determining the de-stressed range. Sur- face boreholes are used to extract gas to relieve pressure in the gob and to study the strata movement in the horizontal direction according to the location of the transverse boreholes. Because the hardness of the strata is quite different in the 12th coal mine, the stress evolution caused by strata hardness is also investigated in this paper.

II. METHODS AND GEOLOGICAL CONDITIONS

Geological conditions and the model

The 12th coal mine of the Pingdingshan coal field is located in the Henan Province in China, and at present, the mining depth is approximately 1000 m. After analyzing a complex of original geo- logical drillings deeper than 1000 m, the rock strata are mainly mudstone, sandstone, and coal. To make the strata histogram much clearer, some unimportant and similar rock strata are combined. In doing so, the key strata that influence the stress evolution and strata movement must first be identified. The strata were sorted into soft and hard, and the non-key strata with similar mechanical properties were assigned to one of the key types. Therefore, the soft key coal seams thicker than 1 m were sorted into the coal seam group, and the hard rock sandstone strata thicker than 10 m were sorted into the sandstone group. The remaining strata are mainly mudstone, with some thin coal seams and thin sandstone strata, and are referred to as the mudstone group. Then, the strata between the adjacent selected soft coal seams and hard sandstone strata were combined. According to geological drilling, a simplified rock strata histogram from the 12th coal mine can be described as shown in Fig. 1.

The strata depth is shown in Fig. 1, and there are six numbered strata in the hard sandstone group and six numbered coal seams. The coal seam #15 is a high-quality coal seam with a high risk of gas emissions, and when the mining depth exceeded 500 m, more than 50 coal and gas outburst accidents occurred. Hence, the coal seam #14, located approximately 12 m above the coal seam #15, was mined first as a protective coal seam. The average thickness of the coal seam #14 is only 0.5 m, but the mined height is 1.8 m; in Fig. 1, the thickness of the coal seam #14 is marked as 1.8 m. The coal seams #8 and #9–10, located approximately 180 m above the coal seam #15, are also prone to dangerous gas outbursts.

To investigate the stress evolution and rock strata movements when mining the coal seams #14 and #15, we built a numerical model using the FLAC3D software, as shown in Fig. 1. The model depth is 1400 m along the *Z*-axis, including all of the selected coal seams, hard sandstone, and other rock strata. The model of the mined panel has a width of 200 m along the *Y*-axis and 800 m along the *X*-axis, which exactly matches the real panel of the 12th coal mine. To reduce the boundary effect, an environment

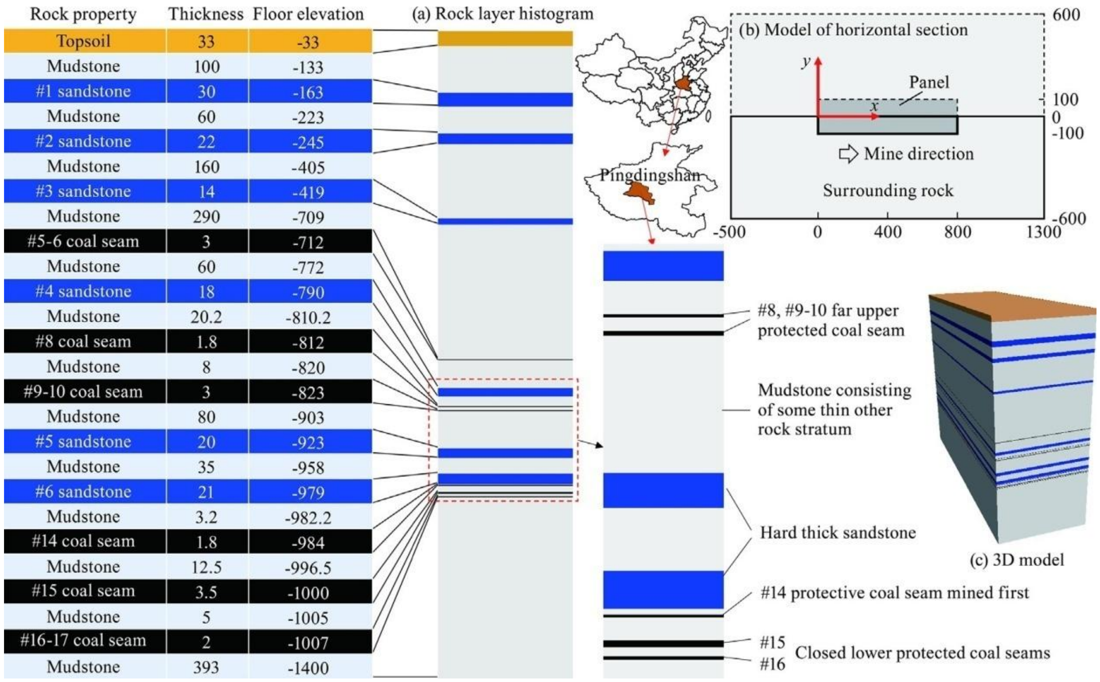

Fig. 1. Geological conditions and the numerical analysis model.

of 500 m is built around the panel, as shown in Fig. 1b. The panel is mined along the *X*-axis, so the numerical model, the stress evolu- tion, and the stratum movement are symmetrical along the *Y*-axis. To reduce the model grids and elements, we can simulate only half of the model, as marked by the solid line in Fig. 1b. Half of the model shown in Fig. 1c consists of 2,877,902 grid cells and 2,808,000 elements, and the numerical model size is the same as in the real state.

Mechanical parameters modelling and validation

The boundary faces of the model are fixed, except for the top face. Fixed grids can only slide along the faces, but the grids cannot leave the faces. The top face represents the earth surface, so the top face is free. The initial stress is isotropic and is applied according to the rock material densities and gravitational acceleration. The mechanical properties of the rocks were tested using standard rock blocks in the laboratory (Table 1), where *E* is the elastic modulus; *P* the Poisson's ratio; *F* the friction angle; *C* the cohesion; *T* the tensile strength; and *D* the density; respectively.

The laboratory parameters are not used directly in the numeri- cal model, because standard rock blocks cannot represent real large-scale rock mass strata. In general, fractures and joints reduce the strength of the rock, so the actual mechanical strength of the rock mass strata will be lower than that of a standard rock block. The laboratory mechanical parameters have to be weakened before they can represent the real rock mass strata. To confirm the accu- racy of the parameters, we use several groups of parameters with different weakness factors to run the model and observe the move- ment of the roof and the floor of the gob. The observation result in the 12th coal mine suggests that the roof and the floor are in con- tact between 20 m and 30 m in the gob. Thus, if during the test the roof and floor are in contact between 20 m and 30 m in the gob, the group of parameters can be assumed to represent the real rock mass. The last parameters of the numerical model shown in Table 1 represent the real rock mass strata as accurately as possible. In the numerical simulation, the roof and the floor contact at approxi- mately 25 m in the gob (Fig. 2), which is much closer to the real condition.

Model execution and monitoring grid setup

The panel in the coal seam #14 was marked as panel #14 and mined as a protective coal seam. The panel was gradually mined from 0 m to 800 m along the *X*-axis. After panel #14 was mined, the high-gas panel #15 in the coal seam #15 was gradually mined from 0 m to 800 m along the *X*-axis. The mining cycle length is 2.5 m when mining both of panels #14 and #15. During the mining process, the displacements of some grids and the ground stresses of some elements just above and below the panel center were con- stantly recorded. The initial 3D coordinates of the monitoring grids are (400, 0, *z*), and the initial 3D coordinates of the monitor ele- ments are (401.25, 1.25, *z*); z represents the depth of the moni- toring point, which may change when the monitoring grids and elements are at different depths.

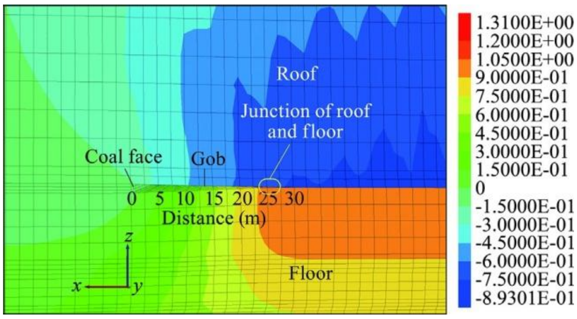

Fig. 2. Strata movement and the rock contact in the gob.

III. RESULTS AND DISCUSSION

Strata movement

Motion trail in the XZ-profile of the monitoring point

The *X*-displacement and *Z*-displacement of the monitoring grids were continuously recorded throughout the mining process. Con- sidering the symmetry of the model, the *Y*-displacement of the strata is very small and can be neglected. The *X*-displacement and *Z*-displacement, according to the same figure, can represent the grid motion trail in the *XZ*-profile. The *X*-displacement is the horizontal movement of the grid, whereas the *Z*-displacement rep- resents the strata sinking.

Fig. 3 shows how the surrounding rock moves during the entire mining process: the strata move both vertically and horizontally. Three symbols are defined in each curve: the first symbol is set when half of the panel #14 is mined, the second symbol is set when the entire panel #14 is mined or at the beginning of panel #15 mining, and the third symbol is set when half of the panel #15 is mined. Thus, the grid motion at different stages can be determined. Fig. 3a–c show the grid above the mined panels, and Fig. 3d shows the grid below the panels.

Z-displacement and expansion rate

The *Z*-axis displacement in Fig. 3 represents a stratum sinking. A large sinking will cause stratum bending and expansion. The grid above the mined panels moves downward, whereas the grid below the panels moves upward. Mining the panel #15 after panel #14 will cause a greater displacement along the *Z*-axis than the mining of panel #14 alone, and the displacement along the *Z*-axis of the grids close to the panel will be larger than those of the distant grids. After panel #15 is mined completely, the strata sinking above 600 m are not large: the maximum sinking at the earth's surface is 265 mm, and the maximum sinking at the depth of 594 m is only 391 mm. This difference in sinking between the strata separated by approximately 600 m is only 126 mm; there- fore, strata above —600 m have an integral settlement without much expansion. The maximum sinking at depths of —710 m, —799 m, —902 m, and —978 m are —525 mm, —717 mm, —2047 mm, and —3005 mm, respectively, so the sinking of strata below —799 m is much larger than that above.

Table 1

Mechanical parameters of standard rock and real rock mass strata.

Parameters Standard rock in labReal rock mass strata

Parameters	Standard rock in lab					Real rock mass strata					
	E (GPa)	*P*	F (°)	*C* (MPa)	*T* (MPa)	*E* (GPa)	*P*	*F* (°)	*C* (MPa)	*T* (MPa)	*D* (kg/m³)
Topsoil	10.2	0.26	26	1.29	0.50	2.1	0.26	19	0.64	0.25	2000
Coal seam	7	0.28	25	0.51	0.20	1.4	0.28	17	0.26	0.1	1350
Mudstone	15.8	0.25	30	1.54	0.60	3.15	0.25	20	0.77	0.3	2600
Sandstone	28	0.2	35	2.57	1.00	5.6	0.2	24	1.29	0.5	2800

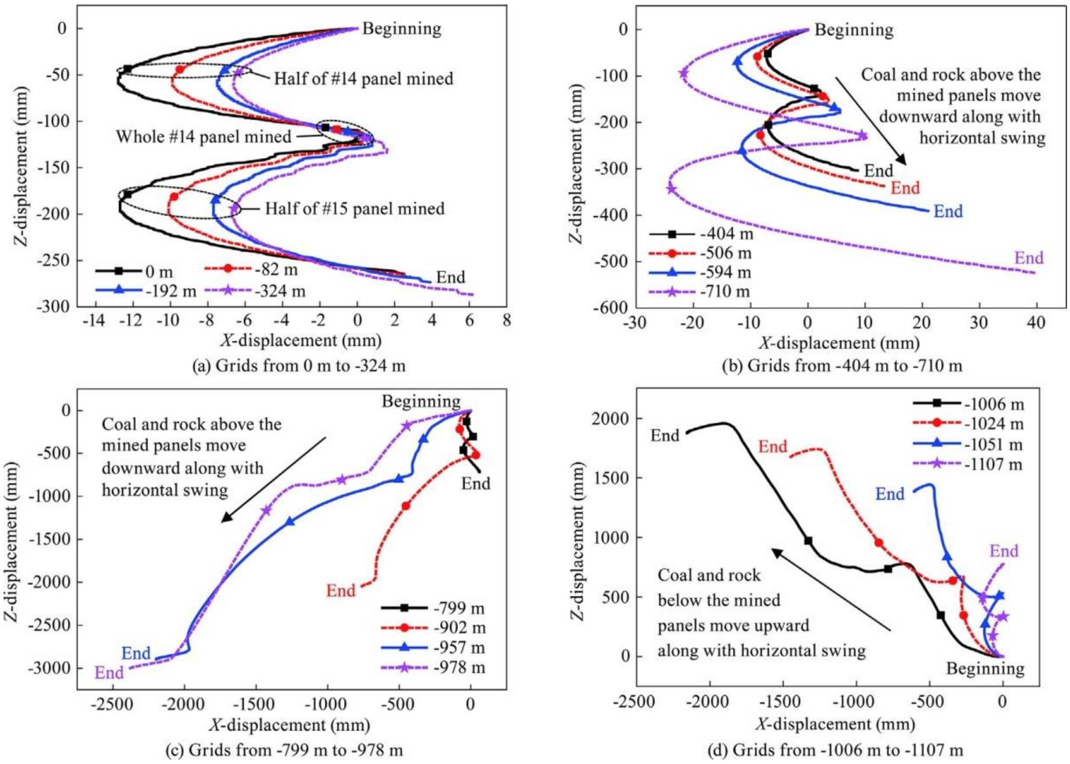

Fig. 3. Trail of motion in the *XZ* profile of the monitoring grids at different depths.

The large difference between the *Z*-displacements of adjacent grids indicates a high expansion rate; the strata expansion rate after the panels #14 and #15, mined at different depths, is shown in Fig. 4.

The expansion rate with depth shows a large difference. In gen- eral, the strata expansion rate is higher closer to the mined panel. A high expansion rate means that the ground stress is greatly reduced. The decreasing stress will generate new gaps and cracks, which is helpful for gas desorption and its flowing away from the coal seam with a high gas content. Consequently, the gas risk of gas emissions will be reduced. In China, the risk of coal seam emis- sion is considered reduced when the stratum expansion rate is higher than 3‰. After panel #14 has been mined, the expansion rates of coal seams #15 and #16 and adjacent rock strata are sub- stantially higher than 3‰, whereas the expansion rates of coal seams #8, #9, and #10 and the adjacent rock strata are less than 3‰. The expansion rate increases greatly when panel #15 is mined after panel #14, and those of coal seams #8, #9, and #10 and the adjacent rock strata are much larger than 3‰.

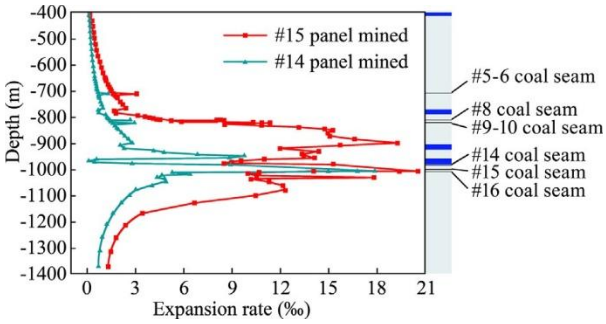

Fig. 4. Expansion rate with depth at different stages.

Fig. 4 also illustrates that rock hardness greatly affects the expansion rate. The expansion rate curve with depth is not smooth: the expansion rates of the sandstone strata are obviously lower than those of the adjacent mudstone strata, and the expan- sion rate of the coal seam is slightly higher than that of the adja- cent mudstone.

Movement in the direction of mining

The *X*-displacement of the monitoring point indicates a hori- zontal movement. Large-scale horizontal movement can easily break down transverse boreholes. Analysis of the horizontal move- ment of rock strata at different depths when mining the panels is critical for determining the transverse borehole arrangement, especially surface boreholes for gas extraction. In Fig. 3, the grids moving towards the negative *X*-direction indicate grids moving towards the gob. The *X*-displacement is much more complex than the *Z*-displacement, and the motion of the grids at different depths is quite different.

The monitored grid points far away from the mined panel swing back and forth, while the grid points close to the panel move directly towards the gob. The range of directional move- ment is disturbed more severely than the swing range. For example, monitoring grids above 799 m and below 1107 m swing back and forth during the process of mining panels #14 and #15: the grids move in the negative *X*-direction when min- ing the initial half of panels #14 and #15, and when the coal face is above monitoring points, the grids move in the positive *X*-direction.

The swing range and directional movement range are not the same when mining panels #14 and #15. For example, monitoring grids at depths of 902 m and 1051 m are at critical depths: the two grids swing back and forth when mining panel #14, but they directly move towards the gob when mining panel #15. Mon- itoring grids at depths between 957 m and 1024 m move towards the gob throughout the entire mining process.

The displacement along the *X*-axis at different depths varies greatly and in a complex manner during the mining process. When the depth is greater than 400 m, the *X*-displacement of the moni- toring grids is greater closer to the mined panel. For example, the maximum *X*-displacement at a depth of 978 m is approximately

2.4 m towards the gob in the final stage, whereas the maximum *X*-displacement at a depth of 404 m is less than 10 mm during the entire mining process. When the depth is less than 324 m, the maximum *X*-displacement decreases with increasing depth. For example, the maximum *X*-displacement of the grid at a depth of 324 m is approximately 6.5 mm towards the gob when half of the panel #15 is mined, whereas the maximum *X*-displacement on the ground surface is approximately 12.5 mm towards the gob when half of panel #15 is mined. The *X*-displacements of the swing grids are, generally, smaller than the grids with directional movement. The swing grids suggest that the rock strata are elastic, the rock stability is high, and the rock was not significantly damaged. The directional movement grids are greatly affected by the mining activity, and rock strata are destroyed and lose their ability to rebound.

An accurate understanding of the rules of rock migration at dif- ferent depths is of great importance for analysis of the de-stressed range and the arrangement of boreholes. Fig. 5a shows the *X*-displacements of the grid points along the normal direction of the panel center at different stages. Five curves represent five stages: the beginning, 400 m of panel #14 mined, 800 m of panel #14 mined, 400 m of panel #15 mined, and the end. The *X*-displacement at the beginning is 0 m, and then the grid points move during the entire mining process. Strata close to the mined panel move more obviously than strata far from the mined panel. Fig. 5b is an enlarged version of Fig. 5a, from which the direc- tional movement range can be easily identified. When mining panel #14, the curves for 400 m and 800 m of mining intersect at two points: the upper point is at a depth of 945 m, and the lower point is at a depth of 1030 m; therefore, the directional move- ment range is in the depth range from 945 m to 1030 m. Based on the same method, the directional movement range is at a depth of 875 m to 1076 m when mining panel #15. In general, the *X*-displacement is so large in the directional movement range that the strata are broken, and the rock carrying capacity decreases, thereby decreasing the stress in this range. In the elasticity range, the horizontal strata movement is similar to that of the horizontal plate motion and collision, which concentrate stress.

Ground stress evolution

The movement of the strata causes a redistribution of stress. The maximum and minimum principal stresses of the monitoring elements in Section 2.3 were continuously recorded throughout the entire mining process, and Figs. 6–9 illustrate the stress evolu- tion. In the four figures, the *X*-coordinates from 0 m to 800 m demonstrate the process of mining panel #14, and those from 800 m to 1600 m demonstrate the process of mining panel #15. The coal face at 400 m suggests that the coal face of panel

#14 is just below or above the monitoring elements, and the coal face at 1200 m suggests that the coal face of panel #15 is just below or above the monitoring elements.

Fig. 6 illustrates the maximum principal stress evolution of the monitoring elements at different depths. The stress changes more significantly when the monitoring element is closer to the panel. The maximum principal stresses generally increase slightly throughout the entire mining process when the depth is less than 803 m. Mining panel #15 after panel #14 yields a higher pressure relief range; for example, the maximum principal stress at a depth of 859 m to 917 m increases when mining panel #14 and decreases when mining panel #15. The maximum principal stress mainly decreases with a depth of more than 954 m. A sharp stress drop mainly follows the stress concentration; for example, the maximum principal stresses of elements at depths of 896 m and 976 m increase when the coal faces approach 400 m and 1200 m, respectively, which is mainly caused by the concentration of abutment stresses, and then the stress decreases in the gob. When the monitoring elements are close to the panels, for exam- ple, at a depth of 976 m, the stress recovers in the gob due to the compaction of the roof and the floor.

The minimum principal stress of different monitoring elements illustrated in Fig. 7 mainly decreases throughout the process of mining panels #14 and #15. The minimum principal stress at depths less than 803 m will not increase as the maximum princi- pal stress does; on the contrary, the minimum principal stress

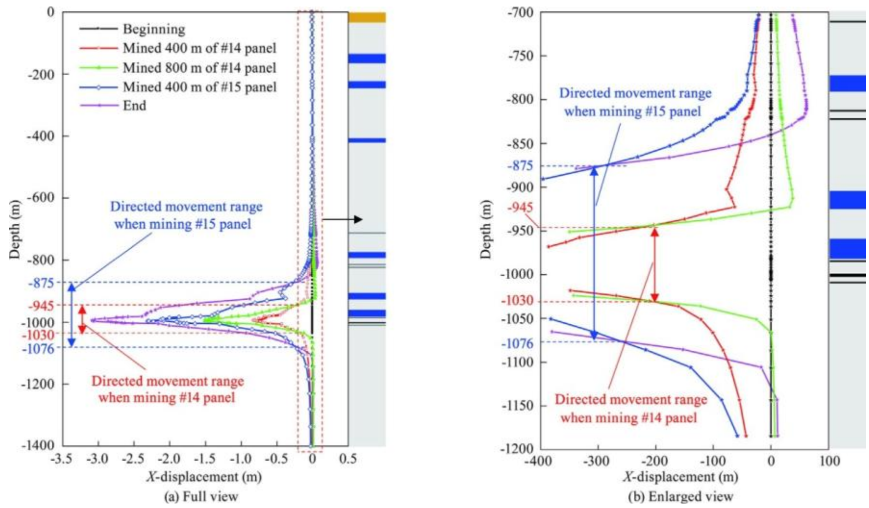

Fig. 5. *X*-displacements of the grids just above or below the panel centre with the depth at different stages.

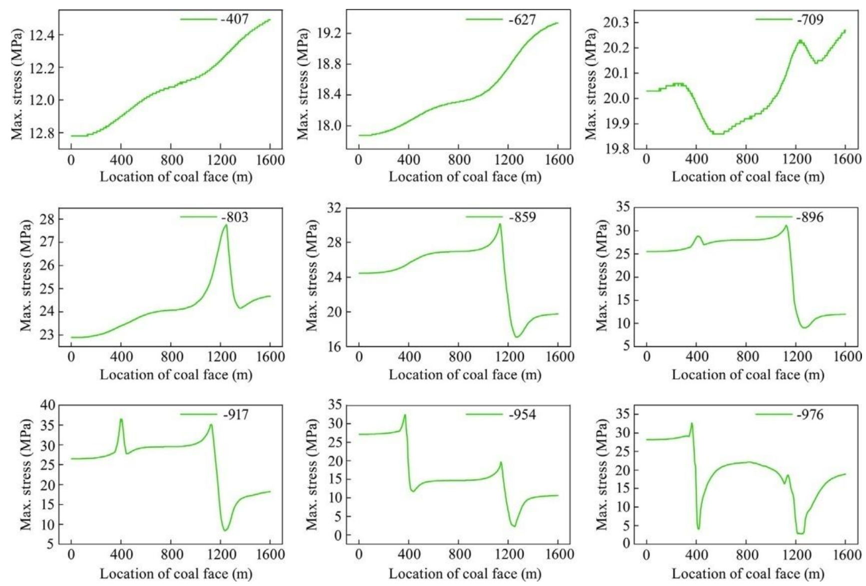

Fig. 6. Maximum principal stress evolution of the monitoring elements above the panels.

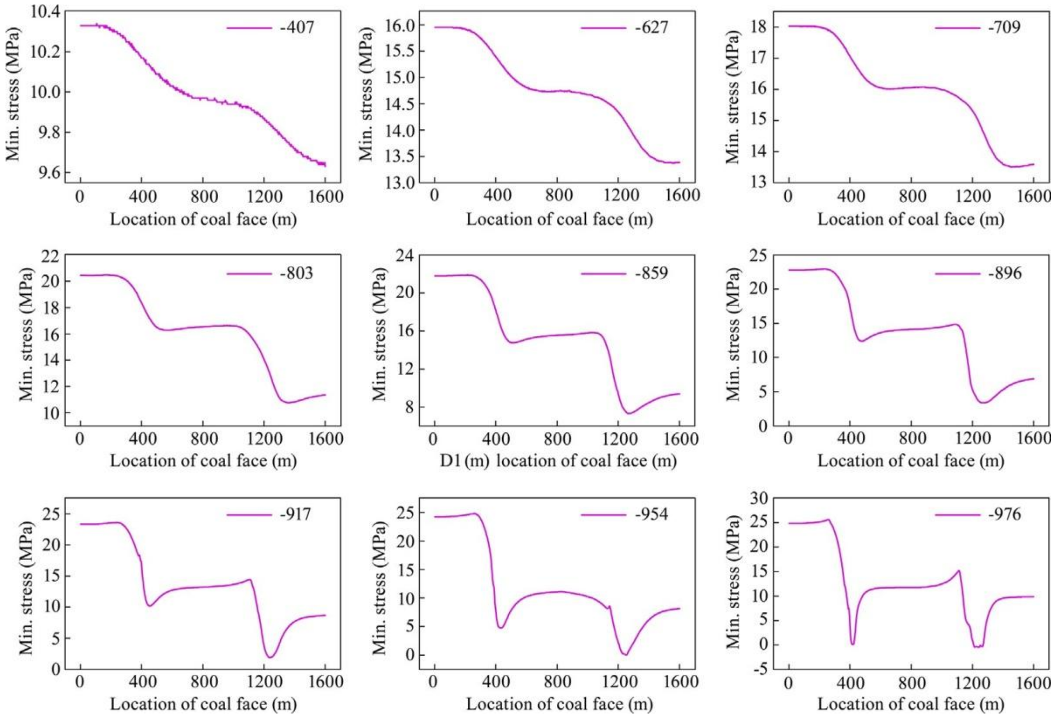

Fig. 7. Minimum principal stress evolution of the monitoring elements above the panels.

decreases throughout the mining process. When the monitoring elements are close to the mined panel, the stress recovery follow- ing a sharp stress drop can also be observed in the gob due to the compaction of the roof and floor. For example, the stress at a depth of 954 m sharply declines when the coal face is close to 400 m or 1200 m, and then the stress gradually recovers in the gob.

Comparing Figs. 6 and 7, the maximum principal stress at depths less than —917 m does not decrease when mining panel #14 alone, whereas the minimum principal stress decreases by more than 10% at a depth of 709 m. Thus, the stress reduction range determined by the minimum principal stress is greater than the maximum principal stress.

The maximum and minimum principal stress evolutions of the monitoring elements below the panels are shown in Figs. 8 and 9, respectively. The stress evolution trends are generally the same as for the elements above the panel.

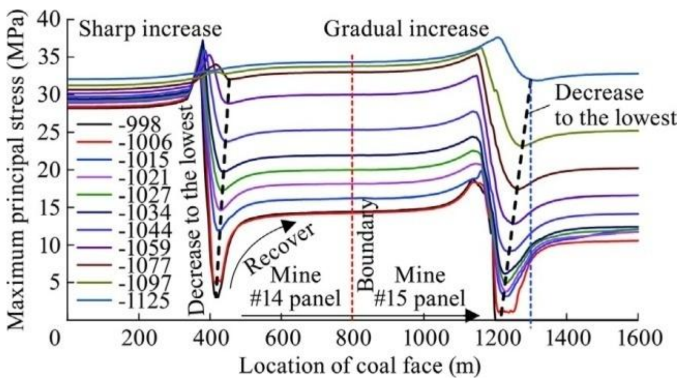

Fig. 8. Maximum principal stress evolution of the monitoring elements below the panels.

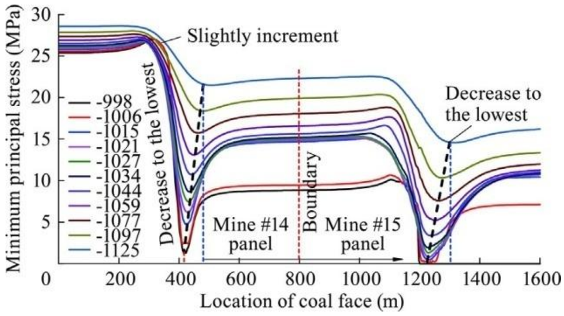

Fig. 9. Minimum principal stress evolution of the monitoring elements below the panels.

By comparing the principal stress at different depths in the same figure, the stress evolution difference can be easily obtained. Similar to the stress evolution above the panel, the stress near the panel is disturbed much more severely. Locations where the min- imum principal stress reaches the lowest value are different at dif- ferent depths. The monitoring elements close to the panel decrease to the lowest value in the gob much earlier. For example, the min- imum principal stress of the stratum at a depth of 1021 m, approximately 21 m below panel #15, decreases to a minimum value when the coal face is located at approximately 20 m, whereas the minimum principal stress of the stratum at a depth of —1125 m, approximately 125 m below panel #15, decreases to a minimum value when the coal face is located at a distance of approximately 100 m. In fact, the time difference of stress relief at different depths also exists on the roof. Gas extraction boreholes for adjacent coal seams should be arranged by considering this time difference to ensure timely and effective gas extraction.

Stress changes dynamically throughout the mining process, and the change trends of the maximum and minimum principal stres- ses at different depths are considerably different. When the strata are far away from the mined panel, the maximum principal stress increases, while the minimum principal stress decreases. When the strata are close to the mined panel, both the maximum and mini- mum principal stresses decrease to the lowest values immediately after the coal face and then gradually recover in the gob.

Stress distribution with depth and the influence of strata hardness

The principal stresses at different depths just above and below the panel center can represent the pressure relief range to some extent. The initial stresses and stresses after mining of panels #14 and #15 were obtained separately. The ratios of the stresses were divided by original stresses, as shown in Fig. 10a and b, respectively. These ratios are used to evaluate the stress decrease and increase ranges.

The directions of the three principal stresses are perpendicular to each other. Fig. 10 shows that stress ratios are different in the three directions. The range in which the three principal stresses have decreased is called the completely de-stressed range. Fig. 10a illustrates that the completely de-stressed range is from a depth of 920 m to 1065 m after mining of panel #14, whereas Fig. 10b illustrates the completely de-stressed range is from a depth of 808 m to 1115 m after mining of panel #15. Mining panel #15 after panel #14, obviously, can increase the completely de-stressed range; the upper range was raised by 112 m, and the lower range was raised by 50 m.

Without a completely de-stressed range, the maximum princi- pal stress generally increases, while the minimum principal stress generally decreases, and the pressure relief effect is obviously worse than in the completely de-stressed range. When the mini- mum principal stress decreases by more than 20% and the maxi- mum principal stress increases, rock strata in the range are called the affected zone. Fig. 10a illustrates that the affected zone is located at a depth from —810 m to —920 m and from —1065 m to —1140 m after panel #14 is mined. Fig. 10b illustrates that the

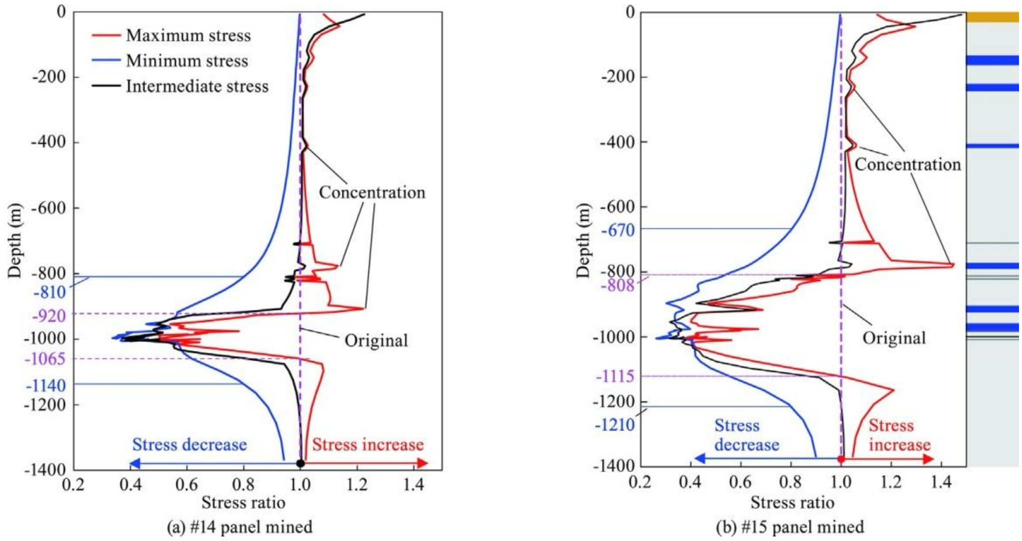

Fig. 10. Principal stress ratio distributions with depth.

affected zones are located at depths from 670 m to 808 m and from 1115 m to 1210 m after panel #15 is mined. The com- pletely de-stressed range and the affected zone after the mining of panel #15 are greatly enlarged compared with the mining of panel #14.

After the panel is mined, the roof sinks and the floor heaves, and the strata near the mined panel have sufficient space to expand, thereby decreasing the vertical and horizontal stress. However, the far away strata can only sink slightly and cannot supply suffi- cient space for the horizontal strata expansion; thus, the horizontal compaction will remain higher than the horizontal stress. Along the normal direction of the panel center, the maximum principal stress is generally along the horizontal direction, and the minimum principal stress is generally along the vertical direction.

Rock hardness greatly affects the maximum principal stress dis- tribution [23]. By scrutinizing the maximum principal stress curve, the maximum principal stress is observed as relatively higher in hard sandstone strata than in adjacent strata, and the maximum principal stress is relatively lower in coal seams than in adjacent rock strata. Stresses deform the soft coal seam relatively easier than the adjacent rock strata, and the deformation transfers some of the stresses originally belonging to the soft coal seam to adja- cent relatively harder rock strata. Because sandstone is much harder than other rock strata, some of the stress of the adjacent rock strata is transferred to the hard sandstone strata.

Stress distribution in the surrounding rock

The maximum principal stress distribution in the *XZ* profile and *YZ*-profile, when panel #14 was mined for 500 m, is illustrated in Fig. 11, and the maximum principal stress distribution, when panel #15 was mined for 500 m, is illustrated in Fig. 12. On the left of the

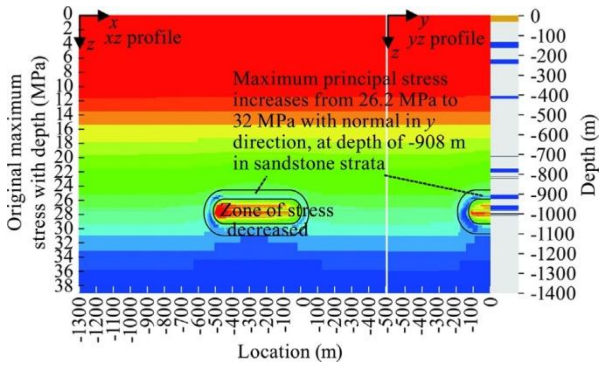

Fig. 11. Maximum principal stress distribution when the #14 panel is mined for 500 m.

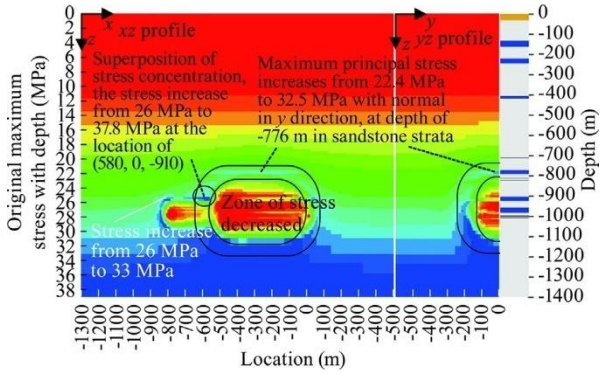

Fig. 12. Maximum principal stress distribution when the #15 panel is mined for 500 m.

figures is the original maximum principal stress distribution with depth, and on the right of the figures is the model depth.

The maximum principal stress close to the coal face decreases substantially in the gob, and then the stress gradually recovers in a deep gob when the roof and floor contact. The stress of the strata close to the mined panel greatly decreases, and the severe stress concentration is located in the de-stressed range. The greatest maximum principal stress concentration is at a depth of 908 m, approximately 75 m above panel #14, after panel #14 is mined. The maximum principal stress increases from 26.2 MPa to 32 MPa with a stress concentration factor of approximately 1.22. The highest stress concentration is located to the right of the hard sandstone stratum #5. The highest maximum principal stress con- centration is at 776 m, approximately 220 m above panel #15, after panel #15 is mined. The maximum principal stress increases from 22.4 MPa to 32.5 MPa, and the stress concentration factor is approximately 1.45. The stress concentration factor when mining panel #15 is greater than in the mining of panel #14.

When mining multiple coal seams, the stress evolution of the coal seam mined later will be affected by a previously mined coal seam. For example, a point (580, 0, 910) is in sandstone stratum #5. The original maximum principal stress is approximately 26 MPa, and the maximum principal stress increased to approxi- mately 32 MPa after panel #14 was mined, up to a maximum of approximately 37.8 MPa after panel #15 was mined for 500 m. When mining panel #15, the location of the maximum stress con- centration is approximately 80 m in front of the coal face and approximately 86 m above panel #15; lastly, the maximum princi- pal stress decreased to approximately 16 MPa when panel #15 was mined.

IV. DISCUSSION

The ground stress increases with depth, which is harmful for gas outburst prevention. Mining a protective coal seam is one of the most effective methods for gas disaster control. Mechanisms of stress redistribution and rock strata movement are critical for determining the pressure relief range and designing the gas extrac- tion boreholes [24].

The results of the study are helpful for organizing the order of coal seam mining in the 12th coal mine and similar coal mines. The risk of gas outburst from coal seam #15 obviously ceases after panel #14 is mined, and the pressure relief range expands signifi- cantly after the mining of panel #15. The upper limit of the com- pletely de-stressed range reaches 808 m after the mining of panel #15, therefore the three principal stresses in coal seams #8 and #9 are reduced. If coal seam #16 is mined after coal seam #15, the completely de-stressed range will again increase. Because coal seams #8 and #9 are far from coal seams #14 and #15, dis- turbed gas in coal seams #8 and #9 cannot flow into the gob of panel #14 or #15 by itself. Therefore, some gas extraction bore- holes should be properly located to extract gas in coal seams #8 and #9 during the process of mining panel #15. The experience in the 12th coal mine in Pingdingshan validates the results: the roadways in coal seam #8 were obviously deformed when mining a panel in coal seam #15, and support difficulty has increased sig- nificantly. The stress applied on the roadway initially increased and then decreased; a change in stress deforms or even breaks the roadway.

In some coal mines, surface borehole drainage technology is applied to extract the pressure relief gas when mining a protective coal seam. Surface boreholes should generally be constructed before the panel is mined, as surface boreholes suffer from rock movement, especially horizontal movement. Large-scale horizon- tal movement can cut off the surface boreholes; hence, surface boreholes must be constructed according to the rock movement characteristics. Boreholes should not enter into the severe distur- bance range, and the well in the elastic swing range must be protected.

The rock stratum hardness significantly affects the stress distri- bution after the coal seam is mined, especially the maximum prin- cipal stress. The maximum principal stress is much lower in the soft coal seam, but much higher in the hard rock strata. Soft strata are usually much more deformable. Hard strata are more difficult to bend, which prevents the sinking of the above rock strata and coal seams. Then the rock mass above has difficulty in expanding and relieving stress, whereas the rock mass below can more easily expand and relieve the stress. Although hard strata are difficult to bend, if the hard rock strata are close to the mined panel, a strong disturbance will bend the hard rock. For example, after panel #14 was mined in the 12th coal mine, a hard sandstone stratum #6 was bent, but hard sandstone #5 and the above strata were not; after panel #15 was mined, hard sandstone strata #5 and #6 were bent, but hard sandstone #4 did not bend. If there are several hard rock strata, the critical plane of the completely de-stressed range and the affected zone is usually one of the hard rock strata, and the location of the critical plane will be affected by the mining depth.

V. CONCLUSIONS

Mining causes complex strata movements. Vertical movement will decrease the vertical stress, and rock bending enhances the rock expansion in the horizontal direction and decreases the hori- zontal stress. Horizontal movement is very different at different depths, causing breaks in transverse boreholes, especially in sur- face boreholes. Boreholes should not be implemented in the severe disturbance zone and should be properly protected.

The hardness of the rock stratum obviously affects the rock movement and the stress distribution. Hard strata contain a greater stress concentration and prevent the above stratum from sinking and de-stressing. Hard strata are helpful for extracting gas and eliminating the outburst risk of the coal seams below; however, they are detrimental to gas extraction and eliminating the outburst risk of the above coal seams.

In the 12th coal mine in Pingdingshan city, the pressure relief range of the upper limit is approximately 200 m after panels #14 and #15 are mined. The gas outburst risk from coal seams #8 and #9–10 is reduced. The proper order of coal seam mining is as follows: #14, #15, #16, #8, and then #9–10.

ACKNOWLEDGMENTS

This study was financially supported by the National Key R&D Program of China (No. 2016YFC0801402), and the National Natural Science Foundation of China (No. 51874291).

REFERENCES

[1]. Iannacchione AT, Tadolini SC. Occurrence, predication, and control of coal burst events in the U.S.. Int J Min Sci Technol 2016;26(1):39–46.
[2]. Li T, Mu Z, Liu G, Du J, Lu H. Stress spatial evolution law and rockburst danger induced by coal mining in fault zone. Int J Min Sci Technol 2016;26(3):409–15.
[3]. Mark C, Gauna M. Evaluating the risk of coal bursts in underground coal mines. Int J Min Sci Technol 2016;26(1):47–52.
[4]. Gu R, Ozbay U. Numerical investigation of unstable rock failure in underground mining condition. Comput Geotech 2015;63:171–82.
[5]. Whittles DN, Reddish DJ, Ren TX. Finite difference continuum modeling of the progressive redistribution of stresses, displacements and shear plane development around an active coal mine longwall. In: Billaux D, Rachez X, Detournay C, Hart R, editors, Finite difference continuum modeling of the progressive redistribution of stresses, displacements and shear plane development around an active coal mine longwall; 2001.
[6]. Dou LM, He XQ, He H, He J, Fan J. Spatial structure evolution of overlying strata and inducing mechanism of rockburst in coal mine. Trans Nonferrous Met Soc China 2014;24(4):1255–61.
[7]. Jiang LS, Mitri HS, Ma NJ, Zhao XD. Effect of foundation rigidity on stratified roadway roof stability in underground coal mines. Arab J Geosci 2016;9:32.
[8]. Xuan DY, Xu JL, Wang BL, Teng H. Borehole investigation of the effectiveness of grout injection technology on coal mine subsidence control. Rock Mech Rock Eng 2015;48(6SI):2435–45.
[9]. Ghabraie B, Ren G, Smith J, Holden L. Application of 3D laser scanner, optical transducers and digital image processing techniques in physical modelling of mining-related strata movement. Int J Rock Mech Min Sci 2015;80:219–30.
[10]. Rezaei M, Hossaini MF, Majdi A. Determination of longwall mining-induced stress using the strain energy method. Rock Mech Rock Eng 2015;48 (6SI):2421–33.
[11]. Song G, Yang S. Investigation into strata behaviour and fractured zone height in a high-seam longwall coal mine. J Southern African Inst Min Metall 2015;115(8):781–8.
[12]. Saghafi A, Pinetown KL. A new method to determine the depth of the de- stressed gas-emitting zone in the underburden of a longwall coal mine. Int J Coal Geol 2015;152(SIA):156–64.
[13]. Shen B. Geotechnical monitoring in coal mining research – case studies. In: Guo W, Shen B, Tan Y, Cheng W, Yan S, editors, Geotechnical monitoring in coal mining research-Case studies; 2013.
[14]. Zhang Q, Zhang J, Kang T, Sun Q, Li W. Mining pressure monitoring and analysis in fully mechanized backfilling coal mining face-A case study in Zhai Zhen Coal Mine. J Central South Univ 2015;22(5):1965–72.

[15]. Li N, Wang E, Ge M, Liu J. The fracture mechanism and acoustic emission analysis of hard roof: a physical modeling study. Arab J Geosci 2015;8 (4):1895–902.
[16]. Trueman R, Lyman G, Cocker A. Longwall roof control through a fundamental understanding of shield-strata interaction. Int J Rock Mech Min Sci 2009;46 (2):371–80.
[17]. Wang W, Cheng Y, Wang H, Liu H, Wang L, Li W, et al. Fracture failure analysis of hard-thick sandstone roof and its controlling effect on gas emission in underground ultra-thick coal extraction. Eng Fail Anal 2015;54:150–62.
[18]. Ju J, Xu J. Structural characteristics of key strata and strata behaviour of a fully mechanized longwall face with 7.0 m height chocks. Int J Rock Mech Min Sci 2013;58:46–54.
[19]. Islam MR, Hayashi D, Kamruzzaman ABM. Finite element modeling of stress distributions and problems for multi-slice longwall mining in Bangladesh, with special reference to the Barapukuria coal mine. Int J Coal Geol 2009;78 (2):91–109.
[20]. Islam MR, Shinjo R. Mining-induced fault reactivation associated with the main conveyor belt roadway and safety of the Barapukuria Coal Mine in Bangladesh: Constraints from BEM simulations. Int J Coal Geol 2009;79 (4):115–30.
[21]. Ghabraie B, Ren G, Zhang X, Smith J. Physical modelling of subsidence from sequential extraction of partially overlapping longwall panels and study of substrata movement characteristics. Int J Coal Geol 2015;140:71–83.
[22]. Zhang P, Peterson S, Neilans D, Wade S, McGrady R, Pugh J. Geotechnical risk management to prevent coal outburst in room-and-pillar mining. Int J Min Sci Technol 2016;26(1):9–18.
[23]. Zhang Y, Stead D, Elmo D. Characterization of strength and damage of hard rock pillars using a synthetic rock mass method. Comput Geotech 2015;65:56–72.
[24]. An F, Cheng Y, Wang L, Li W. A numerical model for outburst including the effect of adsorbed gas on coal deformation and mechanical properties. Comput Geotech 2013;54:222–31.